UNIVERSITY OF MINNESOTA
ST. ANTHONY FALLS HYDRAULIC LABORATORY

Project Report No. 83

Measurements of the Leading-Edge Separation Bubble for Sharp-Edged Hydrofoil Profiles

by
J. M. WETZEL
and
K. E. FOERSTER

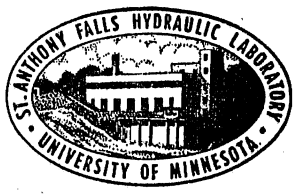

Prepared for
OFFICE OF NAVAL RESEARCH
Department of the Navy
Washington, D.C.
under
Contract Nonr 710(47), Task NR 062-286

June 1966
Minneapolis, Minnesota

ABSTRACT

Measurements were made of the length of the leading edge separation bubble for sharp-edged profiles of finite span submerged below a free surface. These hydrofoils were tested under a fully-wetted flow condition. Flow visualization techniques were used to determine the separation region primarily as a function of velocity, chord length, profile shape, aspect ratio, and angle of attack. The bubble length increased with increasing angle of attack and aspect ratio. An increase in the wedge angle for wedged shaped profiles required an increase in angle of attack to attain the same bubble length. Variation of the chord length and leading-edge thickness had little effect on the ratio of bubble to chord length.

CONTENTS

LIST OF ILLUSTRATIONS

MEASUREMENTS OF THE LEADING-EDGE SEPARATION BUBBLE FOR SHARP-EDGED HYDROFOIL PROFILES

I. INTRODUCTION

The desirability of operating hydrofoil craft at high speeds has led to the design of lifting surface profiles that are relatively efficient under supercavitating conditions. These profiles generally derive their efficiency from the shape of the under (pressure) surface, as the upper (suction) surface is enclosed in the ensuing cavity for this type of operation. The theoretical force coefficients have been found to be in reasonable agreement with the experimental force coefficients as determined in the laboratory. Optimum performance characteristics for a given profile are dependent on the angle of attack which is generally required to be quite low. As the prototype craft will attain high speeds, the cavitation number will be correspondingly low. The low speed capabilities of many test facilities have thus required that the model cavitation number be controlled by adjusting the cavity pressure. This is commonly accomplished by either artificially ventilating the foil with an external gas supply source, or by naturally ventilating the foil to the atmosphere by means of a base-vented strut. Current laboratory experience has indicated that it is difficult if not impossible to attain ventilation inception by either means at low angles of attack.

For the prototype craft during the acceleration period previous to take-off, the foils will probably be operating in a fully wetted flow. The speeds may not be high enough to ensure fully developed cavitation, and thus, it is desirable to attain ventilation at as low a speed as possible for stable operation.

From the present knowledge of the ventilation inception phenomenon, it is necessary that at least two conditions be satisfied; these are:

a. that there be a separated region near the leading edge, and

b. that there be provision of an air port in this region capable of supplying sufficient quantities of air at the proper pressure.

Previous tests in low speed towing tanks have been conducted at relatively large angles of attack to provide a large separated zone encompassing the air supply port or the region near the trailing edge of the base-vented strut. As the angle of attack is decreased, the region of flow separation is also reduced;

thus, it is necessary to supply air to a region extremely close to the leading edge of the foil. As typical supercavitating hydrofoils have a thin leading edge, in practice this becomes difficult to accomplish without disturbing the entire flow field with the injected air. Various schemes have been tried to enhance ventilation inception at low angles of attack and low velocities, with various degrees of success. For example, use has been made of the hysteresis effect by initially setting the angle of attack high to create ventilation inception, and after the cavity has been established, reducing the angle to a lower value. This method proved to be useful in many instances in the laboratory, although it is admittedly circumventing the actual problem of ventilation inception.

Some attempts have been made to assess the thickness and length of the separation bubble on fully wetted hydrofoils by utilizing experimental data taken with a double-wedge profile typically used in supersonic flows [1]*. These data were taken with a two-dimensional foil, and as far as is known, no similar experimental data exist for a sharp-edged hydrofoil of finite span near a free surface. Complete information comparable to that previously obtained in wind tunnels is difficult to obtain for the hydrofoil due to the reduced size of the test body and limitations of the available test facilities. In an attempt to obtain some qualitative information relative to the length of the separation bubble for sharp-edged foils and various flow conditions and thus arrive at conclusions concerning the optimum location of an air port, a series of flow visualization studies were conducted in the Laboratory towing facility. The results of these studies are presented in this report.

II. TYPES OF BOUNDARY LAYER SEPARATION

The type of boundary layer separation that occurs on airfoils or hydrofoils in fully-wetted flow generally falls into three categories: (1) thin airfoil separation (also called long bubble separation) or stall, (2) leading edge stall, and (3) trailing edge stall. The thin airfoil separation is generally observed for sharp leading edge foils, such as supercavitating type foils under fully-wetted flow conditions, and thin, rounded nose airfoil sections. For these foils laminar separation is forced, and thin airfoil stall occurs regardless of the Reynolds number. It is characterized by the separation

---

*Numbers in brackets refer to the List of References on page 15.

of the laminar boundary layer at the leading edge. When the laminar boundary layer subsequently becomes turbulent, it spreads and reattaches itself to the foil surface. In the bubble thus formed under the separated boundary layer, a circulatory flow is set up with the direction of circulation being forward towards the leading edge along the surface of the foil. The foremost part of the bubble near the leading edge is more or less stagnant. The separated zone increases in length as the angle of attack is increased. Although thin airfoil separation has generally been considered as a separation of the laminar boundary layer, flow surveys on a simulated flat plate in a wind tunnel have indicated that turbulent separated flow originated so near the leading edge that no separated laminar flow was detected [3].

The other two categories of airfoil stall were not encountered in the studies described in the present report and are, therefore, mentioned only briefly. Leading edge stall occurs on moderately thick airfoil sections. It appears as a small bubble near the leading edge at some given angle of attack. As the angle of attack is increased, the bubble moves forward towards the leading edge until it suddenly bursts, and the flow becomes separated over the entire chord. The trailing edge stall takes place on very thick sections and is a result of the separation of the turbulent boundary layer near the trailing edge. Further increase in incidence causes the separation point to move towards the leading edge.

Several methods are commonly used in the detection of boundary layer separation: (1) measurement of the pressure distribution over the surface, (2) measurement of the velocity field near the surface, and (3) flow visualization techniques. From pressure distributions, separation is generally characterized by a region of essentially constant pressure followed by a rapid pressure increase. The pressure increases more gradually over the remainder of the chord. The point at which the rapid increase of pressure ends is usually taken as the point of reattachment of the boundary layer. As the separation bubble is very small at small angles of attack, pressure measurements must be made in the immediate vicinity of the leading edge. Unless foils with large chord lengths are used for these studies, the difficulties associated with fabrication of thin sections become considerably amplified.

Direct measurement of the velocity distribution also provides a detailed study of the boundary layer flows. However, perhaps the main disadvantage of

this method is that the tubes used for the velocity probe may influence the flow pattern and therefore modify the boundary layer development.

Flow visualization techniques have proven to be useful in locating regions of flow separation. Various methods are available; however, the following discussion will be limited to the method employing a film of liquid on the surface. If a mixture of oil and some suitable powder is applied to a surface, the mixture will be more or less completely scrubbed from the surface by a non-separated flow. When separation occurs, the mixture will remain in the separated region and the extent of the separation may be estimated. This procedure does not give a detailed description of the separation bubble as the height of the bubble cannot be determined. Only the gross result of the velocity and pressure distributions are indicated by this method. However, it has been found that the liquid film technique does give realistic values for the separated region. It has been reported that by a comparison of the results using flow visualization methods and boundary layer probes, good agreement has been obtained [4]. Where discrepancies were found to exist, more confidence has been placed in the results obtained from the flow visualization methods.

For the studies described in this report, the flow visualization method was adapted as being the most suitable for the particular tests and available facilities.

III. EXPERIMENTAL APPARATUS AND PROCEDURE

A. Towing Facility

The experiments were conducted in the Laboratory towing facility. The towing carriage is capable of attaining speeds up to 25 fps, although the nature of the particular tests generally reduces the maximum speed to about 18 fps to permit a sufficient length of constant velocity test run.

B. Foils

A number of foils of rectangular planform with various profiles, chords, and spans were used for the tests. The foils are listed in the table below.

TABLE I - FOIL CHARACTERISTICS

Foil	Profile	Leading Edge Thickness-in.	Chord-in.	Span-in.	Aspect Ratio	Remarks
A	6° wedge	.002	3	6	2	
B	6° wedge	.002	3	7-1/2	2.5	
C	6° wedge	.018				
D	6° wedge	.035				
E	6° wedge	.053				
F	6° wedge	.003	3	12	4	
G	6° wedge	.003	3	18	6	
H	11° wedge	.008	3	7-1/2	2.5	
I	6° wedge	.004	5	10	2	
J	6° wedge	.004	5	10	2	16° trailing edge flap, flap/chord = 0.25
K	Tulin, C_{L_d} = 0.1	.005	2-1/2	11-1/4	4.5	
L	Tulin, C_{L_d} = 0.1	.005	2-1/2	11-1/4		Circular end plates attached to foil tips
M	Tulin, C_{L_d} = 0.3	.009	2-1/2	11-1/4	4.5	
N	NACA 16-509		3	18	6	

The foils were attached at mid-span to a single supporting strut. This strut was a parabolic base-vented strut for foil A, an 8.5° wedge for foils I and J, and a streamlined shape (NACA 0012) for all other foils.

A definition sketch showing the reference lines for measurement of the angle of attack for wedge and cambered foils is shown in Fig. 1. Note that the nose-tail line was used for cambered foils. The separation bubble of interest is shown as a darkened area near the leading edge of the foils.

C. Procedure for Flow Visualization

The foils were painted black. A mixture of oil and aluminum pigment powder was spread over the upper (suction) surface of the foil with a soft brush using spanwise strokes. The oil medium was SAE 10W, 20, and 30 lubricating oil. The particular oil used was dependent on the water temperature and towing velocity and was selected to generally provide a good pattern during one

test run with a few exceptions. In some cases, duplicate runs were made using different oils. No appreciable changes were generally noted in the flow reattachment points. However, it may be possible that the viscosity of the oil altered the length of very small bubbles, as scatter of the experimental data was found for small bubble lengths. Immediately before the start of the test run, the foil was lowered to the desired depth. Photographs of the flow pattern were taken during the run after a stable pattern had developed. For the cases in which the pattern developed rapidly, photos were taken both at the middle and at the end of the test run. No change in the location of the flow reattachment was observed from these photos. For some of the tests with the foil at a low angle of attack and low velocity, it was necessary to make two test runs before a readily distinguishable pattern was developed.

The above procedure for photographing the flow pattern was modified for foil I. This foil was withdrawn from the water at the end of the test run before photographing. Care was required in that the oil had a tendency to spread out, thus partially obliterating the details of the flow pattern. These effects were minimized by taking the picture immediately after the foil was removed from the water.

IV. DISCUSSION OF RESULTS

A. Typical Flow Patterns

The surface flow patterns were generally photographed at the end of a particular test run. However, much information was obtained by the observer riding the towing carriage relative to the actual development of the flow pattern. It was possible to observe the actual motion of the oil film over the foil and the establishment of the separation bubble and the influence of the tips and strut on the flow characteristics. The results of these observations were extremely useful in the final analysis of the photos.

Some representative photographs of the flow patterns are included for reference purposes. Further discussion of the information extracted from these photos is found in the next section. Some details of the flow pattern have been lost in the reproduction process used for printing. In all of the following photographs, only a half span of the foil suction surface is shown.

The leading edge is at the top and the center supporting strut is at the right hand side of the picture with flow from top to bottom. The foil tip is at the left edge of the photograph.

Fig. 2 shows flow patterns for various aspect ratio foils with a 3-in. chord at an angle of attack of 10° and a velocity of 12 fps. The wedge angle was 6°, and the angle of attack was measured from the underside of the wedge. The reattachment point of the separated flow is located approximately at the 25 per cent chord point on the aspect ratio two foil and increases to about the 60 per cent chord point on the aspect ratio six foil. The heavy accumulation of deposits near the leading edge represents the previously mentioned stagnant region of the separation bubble. The effect of the tip vortex and the influence of the strut on the flow pattern is clearly visible. The appurtenances protruding from the rear halves of the aspect ratio four and six foils are a construction feature of these foils which were originally fabricated for other studies.

In Fig. 3, the effect of the angle of attack on the flow pattern is shown for one particular foil. (The photo for the foil at a relatively large angle of attack was included primarily for illustrative purposes, as the surface flow characteristics are more readily discerned.) At an angle of attack of 8°, the reattachment point is no longer clearly evident. It shows up as a slightly heavier deposit of aluminum particles which were presumably picked up by the separated flow from the accumulation in the stagnant region of the separation bubble and in turn re-deposited at the reattachment point. The effects of the tip vortex become increasingly visible as the angle of attack is increased.

Typical flow patterns for 6° wedge profiles with leading edge thicknesses varying from 0.002 to 0.053 in. are shown in Fig. 4. The leading edges were of semi-circular shape. The most noticeable effect of leading edge thickness appears as an increase in size of the stagnant region as evidenced by a relatively heavy accumulation of oil near the leading edge. The relatively clear areas at the leading edges in some of the photographs are swept clean during the acceleration run before separation is achieved. Because of the stagnant nature of this region, further deposition does not readily take place once a full separation bubble has been achieved unless large amounts of oil deposits are pushed forward. Variation in streak pattern lines result from the different viscosities of oil and aluminum powder concentration used for various tests.

The variation of flow patterns with angle of attack for a wedge angle of 11° is shown in Fig. 5. The profile shape of this wedge is an isosceles triangle so that an additional separation zone is noticeable downstream of the apex at the mid-chord. For $\alpha = 6^{\circ}$, the reattachment point is clearly indicated by the heavier aluminum deposit. However, at the next two angles of attack, the reattachment point is less evident because hardly any excess oil deposits are available at the leading edge for transportation backwards by the separated flow.

The accumulation of a relatively large deposit near the leading edge for many of the foils was of some concern. It was felt that this accumulation might influence the flow pattern and therefore lead to questions concerning the validity of the results. An additional series of tests were thus conducted in which the oil mixture was not applied to the upper surface of the foil in the immediate vicinity of the leading edge. Observation of the resulting flow patterns indicated no appreciable difference in the length of the separation bubble. The accumulation of liquid near the leading edge was, of course, much smaller in these tests, and therefore, it was assumed that no significant errors were introduced from this source.

B. Effect of Foil and Flow Parameters on Bubble Length

1. Aspect Ratio

Bubble lengths were measured from photographs as discussed in the previous section for foils with various aspect ratios. The foils used were foils A, B, F, and G, providing aspect ratios of 2, 2.5, 4, and 6. The chord length was the same (3 in.) for all foils. These results are plotted in Fig. 6 as a function of the angle of attack measured from the underside of the foil. Tests were run for four velocities, and the foils were maintained at a one-chord submergence. In general, the bubble length appears to be shorter for the lower velocity at a given angle of attack and aspect ratio, especially for the larger angles of attack. Very little difference can be noted between the data for velocities of 12 and 16 fps. The length of the bubble was very short at angles of attack less than about 8°, particularly for aspect ratios less than four. As the aspect ratio is increased, the bubble length also increases for the same geometric angle of attack and velocity. It should also be noted that the aspect ratio two foil was supported with a base-vented parabolic strut, whereas the other foils were supported with a streamlined strut. As a result, in Fig. 6a the data at the higher velocities were limited to small

angles of attack. At the higher angles of attack, ventilation from the atmosphere took place sporadically.

This result was unexpected, as the bubble length before ventilation took place was only about 30 per cent of the chord. The trailing edge of the base-vented strut was located at 100 per cent of the chord. Thus, presumably the separated region was not connected to the strut cavity. However, visual observations of the flow for these conditions indicated that the air apparently passed from the strut cavity to the separated region along the unfilleted intersection of the strut and the foil. The interaction of the boundary layers of the strut and foil provided the necessary air path and ventilation immediately occurred.

A more direct comparison of the effect of aspect ratio is shown in Fig. 7a. Data were taken directly from Fig. 6 for a velocity of 16 fps for 3-in. chord foils with aspect ratios of 2.5, 4, and 6. As the data for the aspect ratio two foil were limited to only the smaller angles of attack at a velocity of 16 fps, data were used for an aspect ratio two foil with a 5-in. chord. (It will be shown later that chord length had no influence on the dimensionless bubble length.) It was possible to obtain data with the 5-in. chord foil at higher angles of attack even though this foil also was supported with a base-vented strut. However, the strut for the 5-in. foil was of a wedge shape, whereas the strut for the 3-in. foil was of a parabolic shape. Also, as both foils were submerged at the same submergence ratio, the actual submergence of the 5-in. foil was greater than that for the 3-in. foil. Both of these differences undoubtedly contributed to the particular ventilation behavior mentioned.

The data in Fig. 7a clearly indicate the effect of aspect ratio on bubble length. The greatest differences are noted at the larger geometric angles of attack. The trend of the data for various aspect ratios suggested that the data may be reduced to a common line if the effective angle of attack was used. Lift curve slopes for a 6° wedge of various aspect ratios for a fully-wetted flow were taken from Ref. [2]. The experimental data of Fig. 7a were then referred to the angle of attack for a two dimensional foil and plotted in Fig. 7b. These data for the 6° wedge form a common line, indicating that the effect of aspect ratio can be removed by this procedure. The data from Fig. 6a for foil A at low angles of attack have also been included. By a comparison of the open and filled circles, no effect of chord length can be noted.

With regard to the above mentioned correlation, it should be emphasized that the measurements of the length of the bubble were made in regions away from both the foil tips and the supporting strut. As indicated in the photographs in Section IVA, the influence of the strut and the foil tips may be quite large for some conditions. Therefore, such effects must be also considered in interpretation of the results.

2. Reynolds Number and Wedge Angle

It has previously been noted that the bubble length varied with velocity for the lower velocities. Data for two foils with an aspect ratio of two and chord lengths of 3 and 5 in. are plotted as a function of the Reynolds number based on chord in Fig. 8a. The data for the 3-in. foil are shown with filled symbols, and the data for the 5-in. foil with open symbols. Thus, for a given foil, the variation in Reynolds number was achieved by changing the velocity. More data points are shown for the Type I foil than for the Type A foil, as a wider range of velocities were used in this case. It can be seen that for a given angle of attack, the data for the 3 and 5-in. chord foils are essentially the same, and the bubble length reaches an essentially constant value at the higher Reynolds number. The latter result is apparently in contradiction with aerodynamic data, as Ward [5] reports that a long bubble will diminish with an increase in Reynolds number, until eventually a short separation bubble is attained.

The effect of wedge angle on bubble length is shown in Fig. 8b for two wedges with an aspect ratio of 2.5 and a 3-in. chord. Only the data for velocities of 4 and 16 fps have been plotted. The 11° wedge had a different shape in that it was in the form of an isosceles triangle rather than the simple wedge form as used for the 6° wedge foils. For the 11° wedge, a larger angle of attack was required to obtain the same bubble length than for the 6° wedge. Such a behavior has also been previously mentioned by Barr [1], where he made a prediction based on limited data for airfoils that the angle of attack for a given bubble size increases with wedge angle.

3. Flap Angle

A brief series of tests were conducted to determine the influence of a deflected trailing edge flap on the length of the separated region. These tests were carried out with a 6° wedge foil of 5-in. chord (Foils I and J), whereas previous tests were conducted with 3-in. chord foils.

For reference purposes, tests were first made with the foil having a zero degree flap angle. The results for four velocities are shown in Fig. 9a. These data are similar to those for the foil with a smaller chord length in that the bubble lengths for the 12 and 16 fps velocities are essentially the same. The data for the foil with a 16° flap (flap-chord ratio of 0.25) are shown in Fig. 9b. By comparison of Figs. 9a and b, it can be seen that the effect of the flap is to lengthen the separation bubble, particularly for the larger angles of attack. Not much difference in bubble length has been observed at the small angles of attack; however, the bubble lengths for this condition were extremely small in any case and difficult to determine with much accuracy.

4. Camber

A series of tests were run using cambered foils with sharp and rounded leading edges. The foils used for these tests were modified Tulin-Burkhart profiles and also a NACA 16-509 profile, as these foils were readily available from previous experimental programs. Data for cambered foils with a design lift coefficient of 0.1 are shown in Figs. 10a and b. The Type L foil in Fig. 10b consisted of the same foil fitted with large circular plates at the tips to reduce the effects of finite span. The same general trends of the data are observed as were previously discussed for the wedge profiles. Only small differences were found in the bubble lengths for the two foils. Data for a cambered foil with a design lift coefficient of 0.3 and an aspect ratio of 4.5 are shown in Fig. 10c. For smaller angles of attack, the bubble length was about the same for both the smaller and larger cambered foils. At larger angles of attack, the separation bubble was shortened as the camber was increased. It should be noted that the angle of attack was referred to the nose-tail line in all cases. If the angle of attack would have been referred to the reference line, the ordinate for the $C_{L_d} = 0.3$ foil would be reduced more than than the ordinate for the $C_{L_d} = 0.1$ foil, however, the same general trend would still exist although to a lesser degree.

Some data were also taken with a NACA 16-509 section typically used for non-cavitating flows. The results are plotted in Fig. 10d for four velocities. The general shape of the curves is the same as for the other profiles previously discussed, although this section had a much larger leading edge radius than any of the other profiles.

5. Leading Edge Thickness

It was of interest to briefly investigate the effect of leading edge thickness on separation for a particular profile. The profile selected was a 6° wedge of aspect ratio 2.5, as it was possible to easily vary the nose-radius for this shape by cutting back and reshaping the leading edge. The results are shown in Fig. 11 for various angles of attack and velocities. The data are plotted in a slightly different form than previously used in an attempt to better illustrate the general trends. For essentially all velocities and angles of attack, the bubble length increased slightly as the leading edge thickness was increased. It was originally anticipated that a much larger change would be found, as the magnitude of the velocity peak on the upper surface is proportional to incidence and nose radius. Barr has shown for airfoil sections that the increment of local velocity due to incidence was reduced quite rapidly as the nose radius was increased.

C. Air Injection into Separated Region

In previous tests with forced-ventilated foils at this Laboratory, ventilation at lower angles of attack was achieved by injecting air near the leading edge at the centerline of the foil. It was possible to obtain a stable cavity at an angle of attack of 7° for a velocity of 12 fps. If the angle was reduced to 6°, sporadic air pockets were observed along the leading edge. A full cavity no longer existed. With knowledge of the extent of boundary layer separation on the sharp-edged profiles, a few tests were carried out to determine whether or not air injection into this region would result in a well defined and stable cavity. Modifications were made to foil B to incorporate various systems of air injection.

Two additional tubes were placed on the upper surface of the foil so that a small quantity of air was blown toward the leading edge. It was found that ventilation was poorer than in the previous case, perhaps due to a disruption of the normal flow pattern by the additional air jets. To further investigate this effect, a thin-walled tube was flattened and located about 0.2 in. behind and parallel to the leading edge. A number of holes were drilled into this tube for blowing air towards the leading edge. Again, full ventilation was not observed until the angle of attack exceeded about 10°. It thus appears that the addition of a small quantity of air near the leading

edge through a very narrow opening at the foil centerline may have been the best method of attaining ventilation inception at low velocities.

V. CONCLUSIONS

Based on the results of the flow visualization studies, the following statements may be made concerning the length of the leading edge separation bubble for fully-wetted, sharp-edged profiles:

1. At low angles of attack, the separated region was very small, or could not be observed. For all profiles tested, an increase in angle of attack resulted in an increase in length of the bubble.

2. Bubble length increased with velocity for the smaller angles of attack until an essentially constant length was attained at the higher velocities. The bubble length divided by the foil chord was constant at the smaller angles of attack for chordal Reynolds numbers greater than 4×10^5.

3. For a given geometric angle of attack, the bubble length increased with foil aspect ratio. The ratio of the bubble length to the foil chord was essentially independent of chord length for a given velocity. Influence of the foil tips on the boundary layer flow can be quite large for certain conditions. Through consideration of the effective angle of attack, effects of aspect ratio could be removed.

4. Variation of the leading edge thickness for a particular profile had minor effect on the bubble length, although a slight increase in length was noted with the thicker leading edge.

5. Deflection of a trailing edge flap tended to increase the bubble length, particularly for the larger angles of attack.

6. An increase in wedge angle resulted in a larger angle of attack being required to obtain the same bubble length.

7. Various schemes of introducing air into the region of the leading edge bubble at low angles of attack have met with limited success. Best results were obtained by injecting air forward of the leading edge of the supporting strut.

LIST OF REFERENCES

[1] Barr, R. A., Ventilation Inception, Hydronautics, Inc., Laurel, Md., Technical Report 127-4, March 1963.

[2] Kermeen, R. W., Experimental Investigations of Three-Dimensional Effects on Cavitating Hydrofoils, California Institute of Technology, Eng. Div., Pasadena, California, Rpt. No. 47-14, September 1960.

[3] Gault, Donald E., An Investigation at Low Speed of the Flow over a Simulated Flat Plate at Small Angles of Attack using Pitot-Static and Hot-Wire Probes, NACA TN 3876, March 1957.

[4] Gault, Donald E., Boundary-Layer and Stalling Characteristics of the NACA 63-009 Airfoil Section, NACA TN 1894, June 1949.

[5] Ward, Julian W., "The Behavior and Effects of Laminar Separation Bubbles on Aerofoils in Incompressible Flow," Journal of the Royal Aeronautical Society, Vol. 67, December 1963, pp. 783-790.

F I G U R E S

(1 through 11)

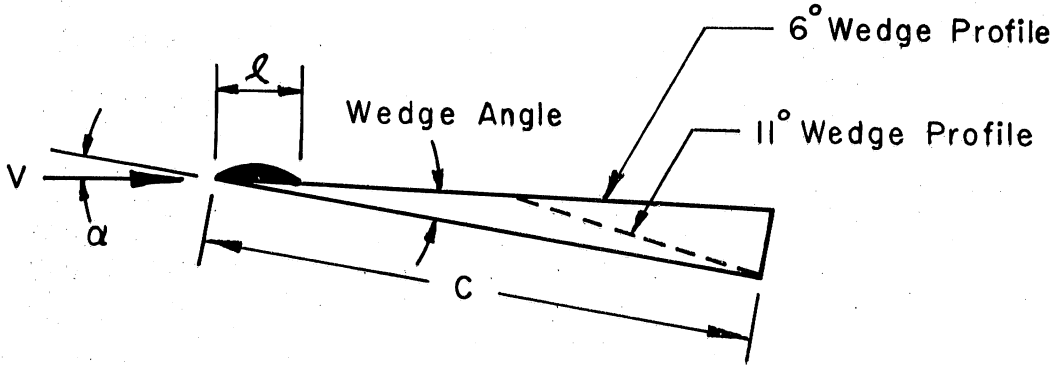

(a) Wedge Foils

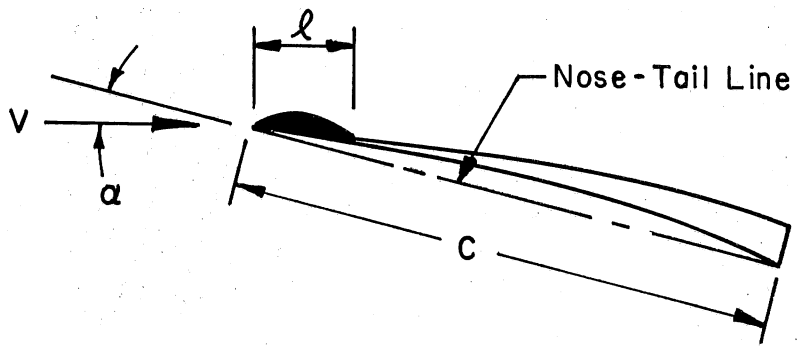

(b) Cambered Foil

Fig. 1 - Definition Sketch

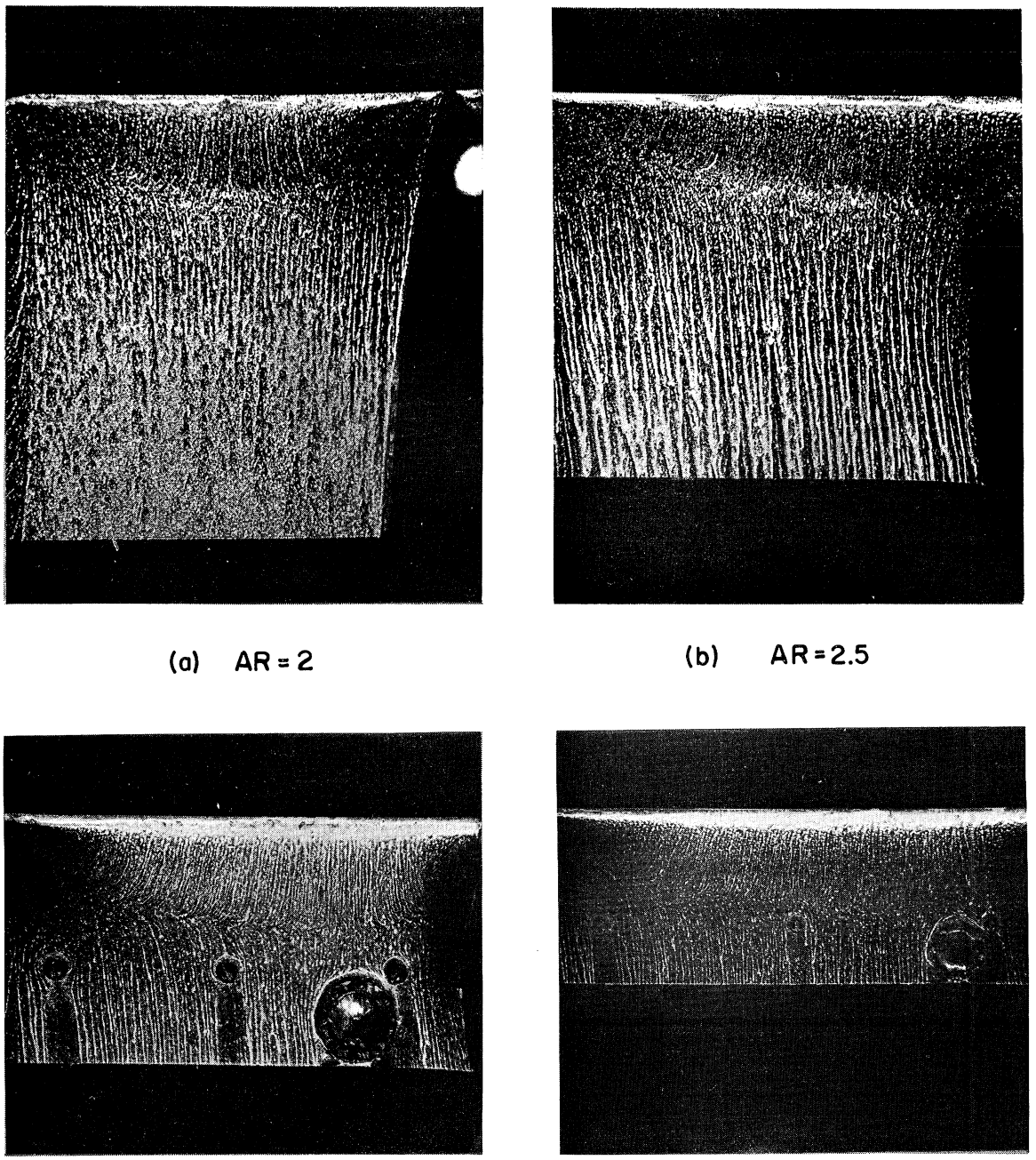

Fig. 2 - Typical Flow Patterns for Foils of Various Aspect Ratios, 6 Degree Wedge

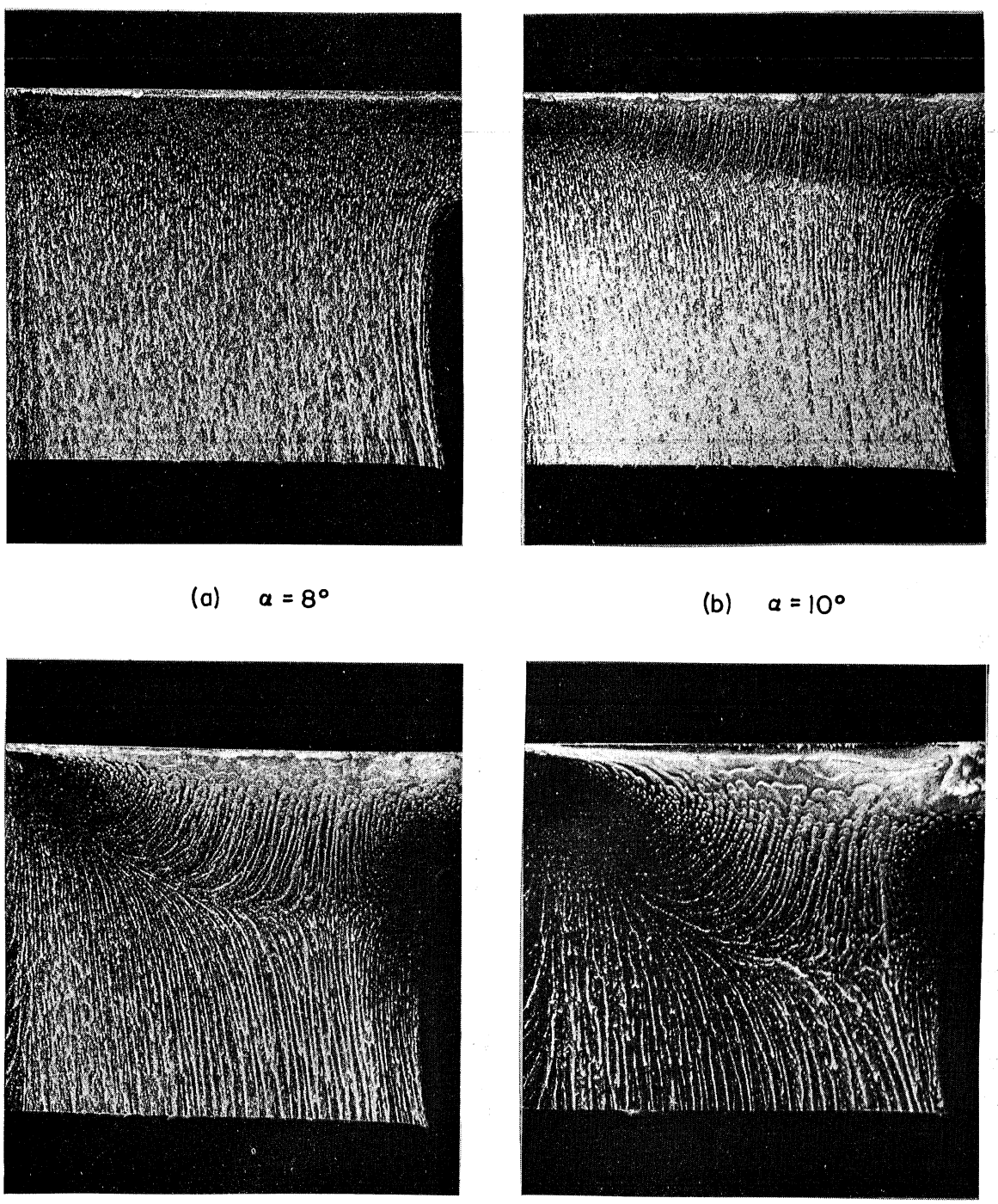

Fig. 3 - Typical Flow Patterns for Foil B at Various Angles of Attack

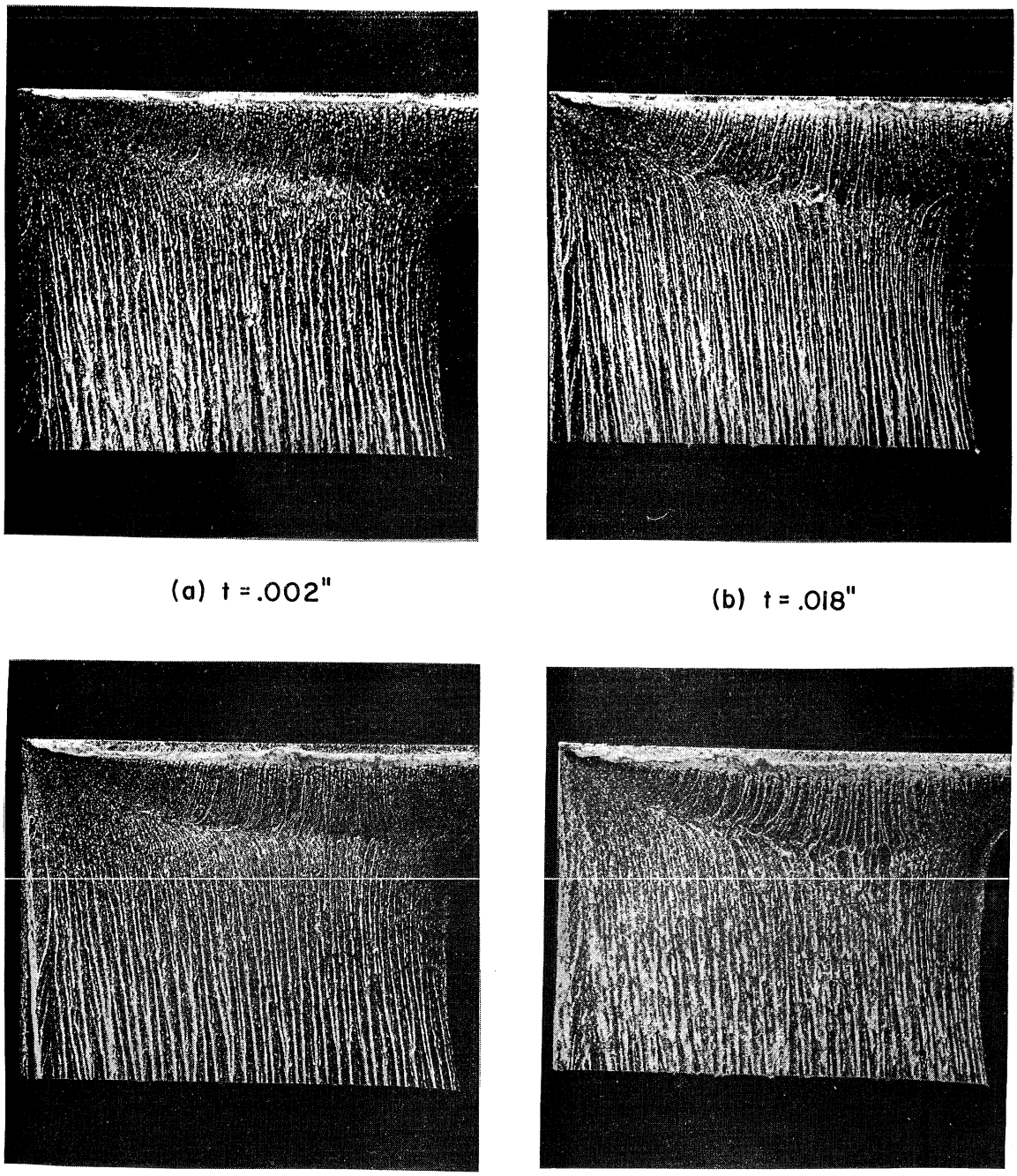

Fig. 4 - Typical Flow Patterns Showing Effect of Leading Edge Thickness, Foils B, C, D, and E

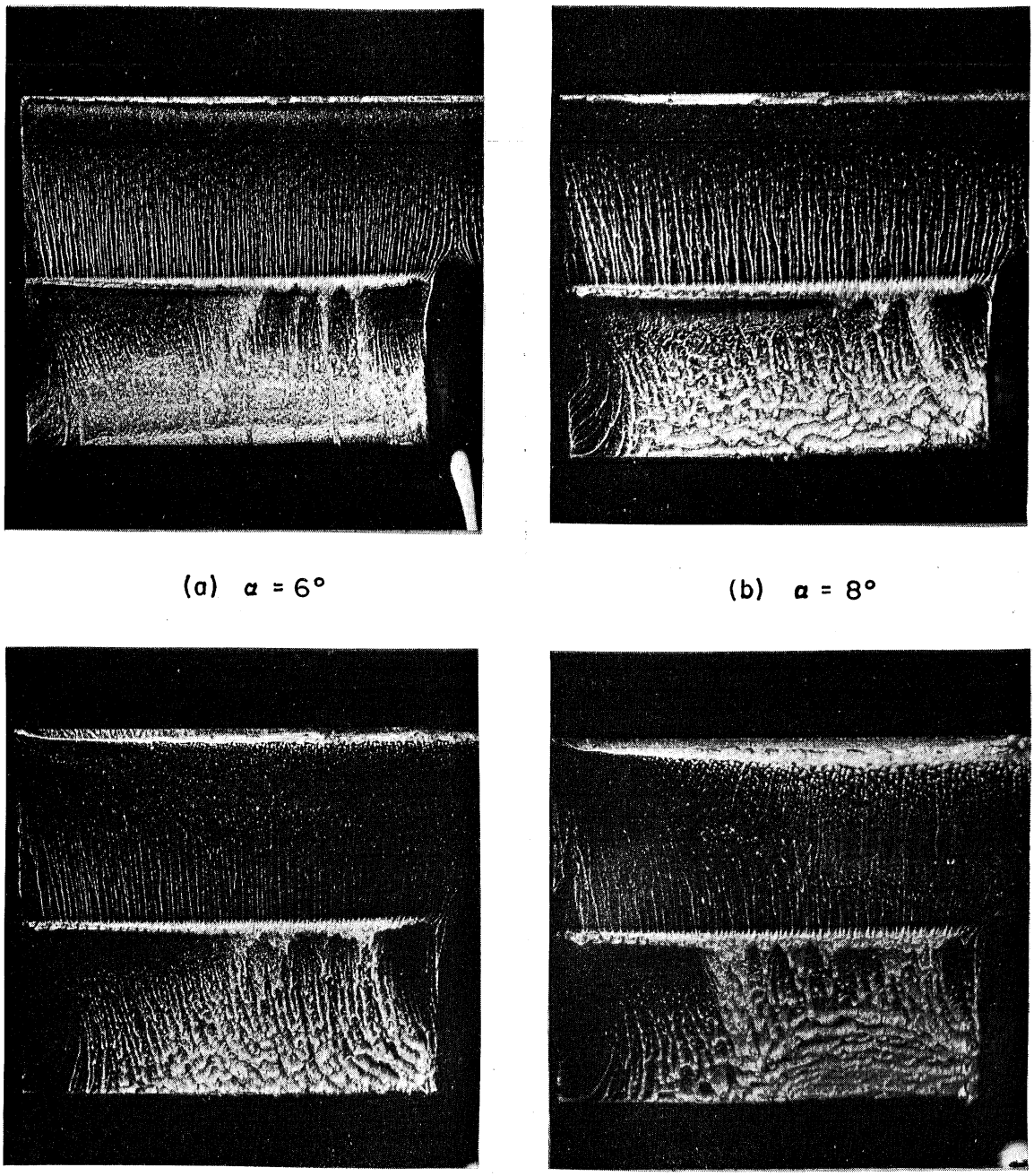

(a) $\alpha = 6°$

(b) $\alpha = 8°$

(c) $\alpha = 10°$

3"x7.5"x11° Wedge

(d) $\alpha = 12°$

V=16 fps

Fig. 5 - Flow Patterns for Foil H at Various Angles of Attack

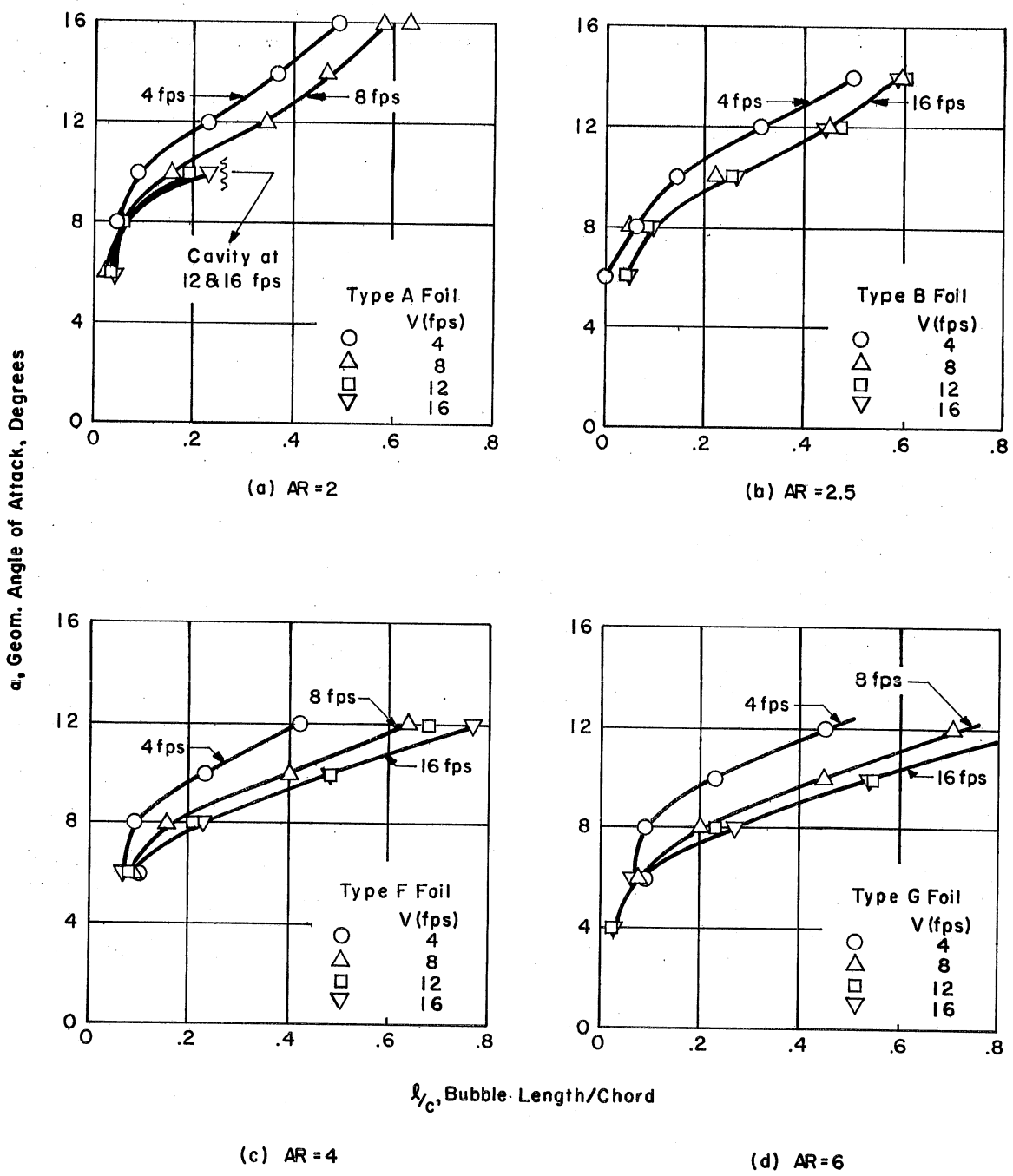

Fig. 6 - Variation of Bubble Length with Aspect Ratio for a 6 Degree Wedge

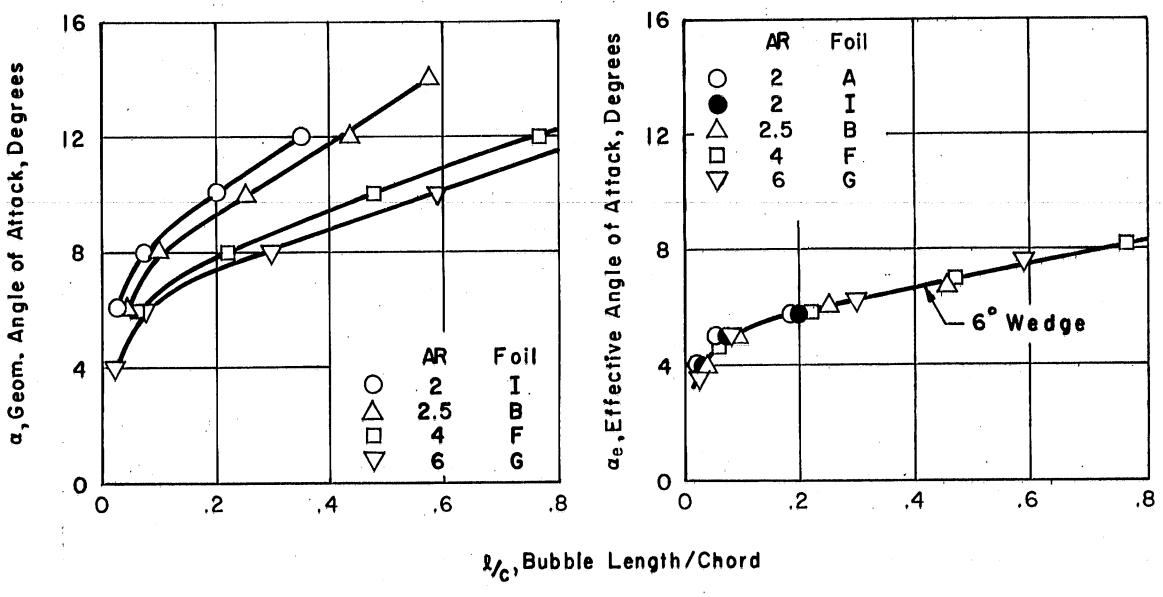

(a) Effect of Aspect Ratio (b) Aspect Ratio Correction

Fig. 7 - Comparison of Data for Various Aspect Ratios, V = 16 fps

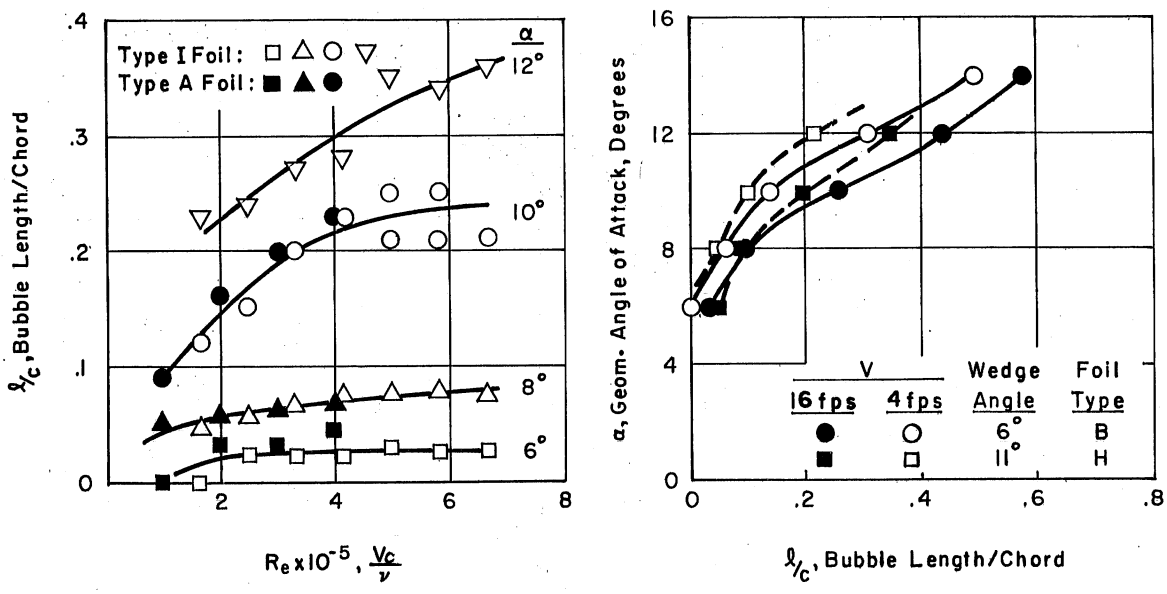

(a) Effect of Reynolds No. (b) Effect of Wedge Angle

Fig. 8 - Variation of Bubble Length with Reynolds Number and Wedge Angle

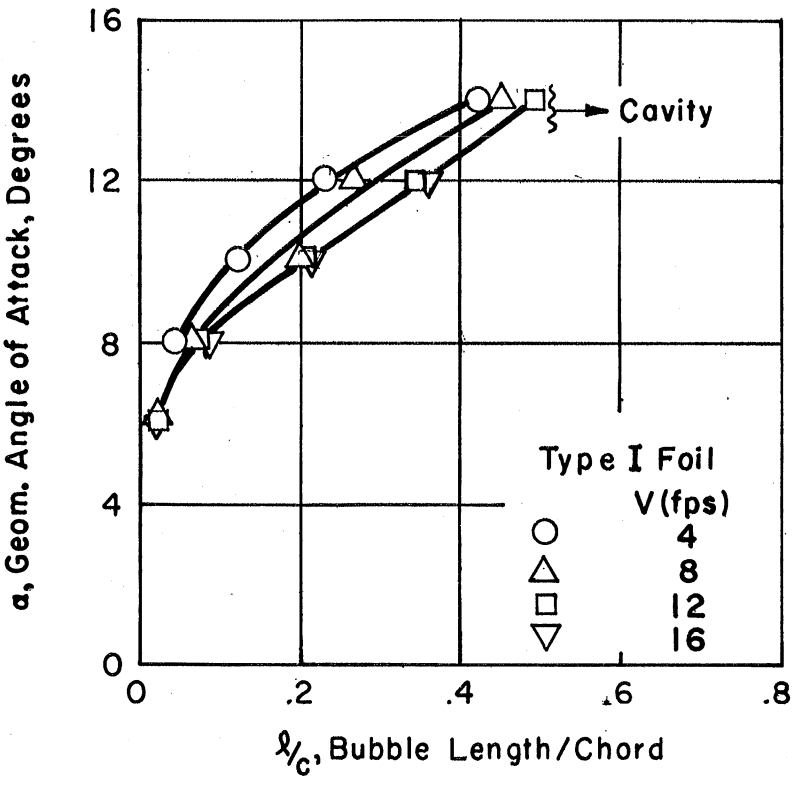

(a) Flap Angle = 0°

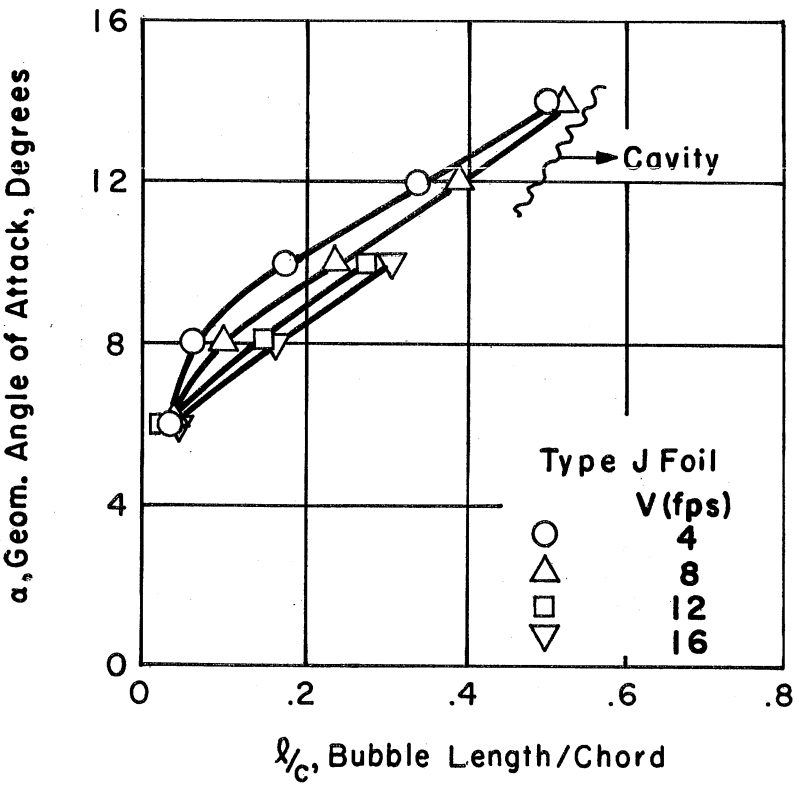

(b) Flap Angle = 16°

Fig. 9 - Bubble Length on a 6 Degree Wedge of Aspect Ratio 2 with a Trailing Edge Flap

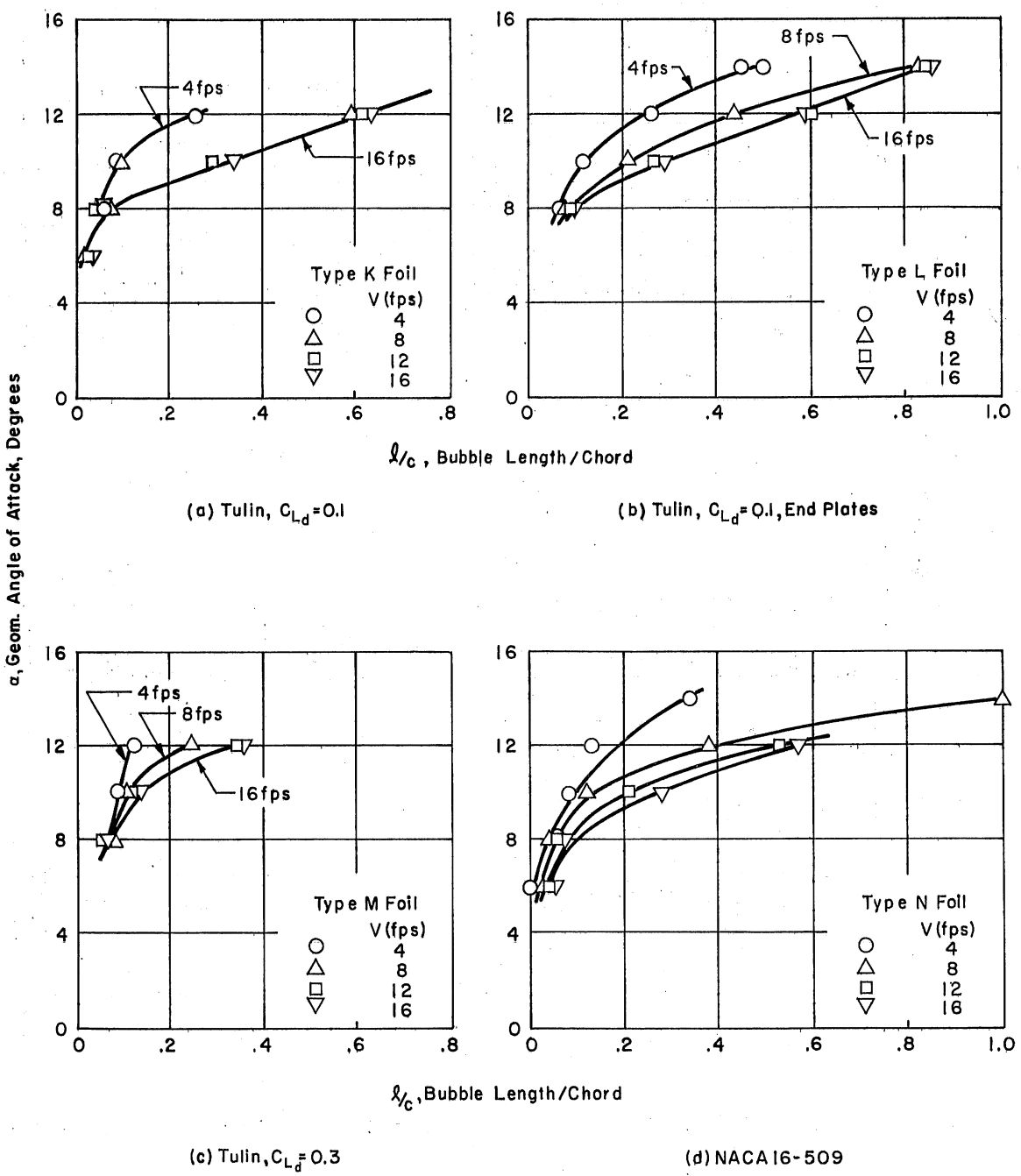

Fig. 10 - Bubble Length for Cambered Foils with Sharp and Rounded Leading Edges

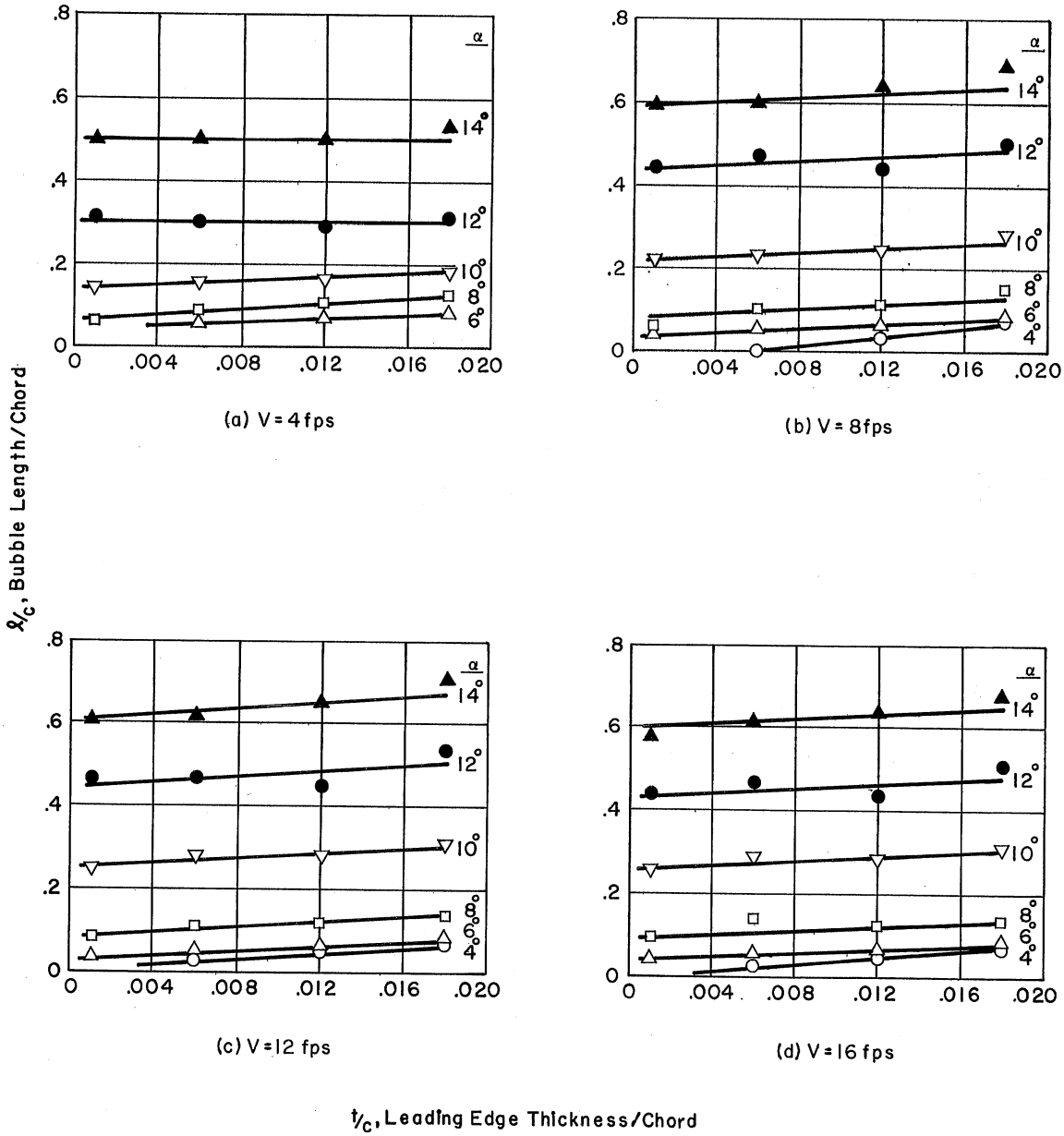

Fig. 11 - Effect of Leading Edge Thickness on Separation for a 6 Degree Wedge of Aspect Ratio 2.5

DISTRIBUTION LIST FOR PROJECT REPORT NO. 83

of the St. Anthony Falls Hydraulic Laboratory

Copies	Organization
6	Chief of Naval Research, Department of the Navy, Washington, D. C., 20360, Attn: 3 - Code 438 1 - Code 461 1 - Code 463 1 - Code 466
1	Commanding Officer, Office of Naval Research, Branch Office, 495 Summer Street, Boston 10, Massachusetts.
1	Commanding Officer, Office of Naval Research, Branch Office, 219 S. Dearborn St., Chicago, Illinois 60604.
1	Commanding Officer, Office of Naval Research, Branch Office, 207 West 24th Street, New York 11, New York.
25	Commanding Officer, Office of Naval Research, Branch Office, Box 39, Fleet Post Office, New York, New York 09510.
1	Commanding Officer, Office of Naval Research, Branch Office, 1030 East Green Street, Pasadena 1, California.
1	Commanding Officer, Office of Naval Research, Branch Office, 1000 Geary Street, San Francisco 9, California.
6	Director, Naval Research Laboratory, Washington 25, D. C., Attn: Code 2027.
3	Chief, Bureau of Naval Weapons, Department of the Navy, Washington 25, D. C., Attn: 1 - Code RRRE 1 - Code RAAD 1 - Code RAAD-222
7	Chief, Bureau of Ships, Department of the Navy, Washington 25, D. C. Attn: 1 - Code 312 1 - Code 335 1 - Code 420 1 - Code 421 1 - Code 440 1 - Code 442 1 - Code 449
1	Chief, Bureau of Yards and Docks, Department of the Navy, Washington 25, D. C. Attn: Code D-400.

Copies	Organization
12	Commanding Officer and Director, David Taylor Model Basin, Washington 7, D. C., Attn: 1 - Code 500 1 - Code 513 1 - Code 520 1 - Code 525 1 - Code 526 1 - Code 526A 1 - Code 530 1 - Code 533 1 - Code 580 1 - Code 585 1 - Code 589 1 - Code 700
1	Commander, Naval Ordnance Test Station, China Lake, California, Attn: Code 753.
1	Commander, Naval Ordnance Test Station, Pasadena Annex, 3202 E. Foothill Boulevard, Pasadena 8, California, Attn: Code P508.
1	Commander, Portsmouth Naval Shipyard, Portsmouth, New Hampshire, Attn: Planning Department.
1	Commander, Boston Naval Shipyard, Boston, Massachusetts, Attn: Planning Department.
1	Commander, Pearl Harbor Naval Shipyard, Navy No. 128, Fleet Post Office, San Francisco, California, Attn: Planning Department.
1	Commander, San Francisco Naval Shipyard, San Francisco, California, Attn: Planning Department.
1	Commander, Mare Island Naval Shipyard, Vallejo, California, Attn: Planning Department.
1	Commander, Puget Sound Naval Shipyard, Bremerton, Washington, Attn: Planning Department.
1	Commander, Philadelphia Naval Shipyard, Philadelphia, Pennsylvania, Attn: Planning Department.
1	Commander, Norfolk Naval Shipyard, Portsmouth, Virginia, Attn: Planning Department.
1	Commander, Charleston Naval Shipyard, Charleston, South Carolina, Attn: Planning Department.
1	Commander, Long Beach Naval Shipyard, Long Beach 2, California, Attn: Planning Department.
1	Commander, US Naval Weapons Laboratory, Dahlgren, Virginia, Attn: Planning Department.

Copies	Organization
1	Commander, US Naval Ordnance Laboratory, White Oak, Maryland.
1	Commander, US Naval Weapons Laboratory, Dahlgren Virginia, Attn: Computation and Exterior Ballistics Laboratory (Dr. A. V. Hershey).
1	Superintendent, US Naval Academy, Annapolis, Maryland, Attn: Library.
1	Superintendent, US Naval Postgraduate School, Monterey, California.
1	Commandant, US Coast Guard, 1300 E Street, NW, Washington, D. C.
1	Secretary, Ship Structure Committee, US Coast Guard Headquarters, 1300 E Street, NW, Washington, D. C.
1	Commander, Military Sea Transportation Service, Department of the Navy, Washington 25, D. C.
1	Division of Ship Design, Maritime Administration, 441 G Street, NW, Washington 25, D. C.
1	Superintendent, US Merchant Marine Academy, Kings Point, Long Island, New York, Attn: Captain L. S. McCready.
1	Commanding Officer and Director, US Navy Mine Defense Laboratory, Panama City, Florida.
1	Commanding Officer, NROTC and Naval Administrative Unit, Massachusetts Institute of Technology, Cambridge 39, Massachusetts.
1	Commander, Hdqs. US Army Transportation Research and Development Command, Transportation Corps, Fort Eustis, Virginia, Attn: Marine Transportation Division.
1	Air Force Office of Scientific Research, Mechanics Division, Washington 25, D. C.
1	Commander, Wright Air Development Division, Aircraft Laboratory, Wright-Patterson Air Force Base, Ohio, Attn: Mr. W. Mykytow, Dynamics Branch.
1	Director of Research, Code RR, National Aeronautics and Space Administration, 600 Independence Avenue, SW, Washington, D. C. 20546.
1	Director, Langley Research Center, Langley Station, Hampton, Virginia, Attn: Mr. I. E. Garrick.
1	Director, Langley Research Center, Langley Station, Hampton, Virginia, Attn: Mr. D. J. Marten.
1	Director, Engineering Science Division, National Science Foundation, Washington, D. C.
1	Director, National Bureau of Standards, Washington 25, D. C., Attn: Mr. J. M. Franklin.

Copies	Organization
1	Dr. G. B. Schubauer, Fluid Mechanics Section, National Bureau of Standards, Washington 25, D. C.
20	Defense Documentation Center, Cameron Station, Alexandria, Virginia.
1	Office of Technical Services, Clearinghouse, 5285 Port Royal Road, Springfield, Virginia 22151.
1	Mr. Alfonso Alcadan L., Director, Laboratorio Nacional de Hydraulica, Antiguo Camino A Ancon, Casialla Postal, 682, Lima, Peru.
1	Mr. T. A. Duncan, Lycoming Division, AVCO Corporation, 1701 K Street, NW, Apartment 904, Washington, D. C.
1	Baker Manufacturing Company, Evansville, Wisconsin.
1	Professor S. Siestrunck, Bureau D'Analyse et de Recherche Appliquees, 47, Avenue Victor Cresson, Issy-les-Moulineaux, Seine, France.
1	Professor A. Acosta, California Institute of Technology, Pasadena 4, California.
1	Professor M. Plesset, California Institute of Technology, Pasadena 4, California.
1	Professor T. Y. Wu, California Institute of Technology, Pasadena 4, California.
1	Professor A. Powell, University of California, Los Angeles, California.
1	Dr. Maurice L. Albertson, Professor of Civil Engineering, Colorado State University, Fort Collins, Colorado 80521.
1	Professor J. E. Cermak, Colorado State University, Department of Civil Engineering, Fort Collins, Colorado.
1	Dr. Blaine R. Parkin, AiResearch Manufacturing Company, 9851-9951 Sepulveda Boulevard, Los Angeles 45, California.
1	Robert H. Oversmith, Chief of ASW/Marine Sciences, Mail Zone 6-107, General Dynamics - Convair, San Diego, California 92112.
1	Dr. Irving C. Statler, Head, Applied Mechanics Department, Cornell Aeronautical Laboratory, Inc., P.O. Box 235, Buffalo, New York 14221.
1	Mr. Richard P. White, Jr., Cornell Aeronautical Laboratory, 4455 Genesee Street, Buffalo, New York.

Copies	Organization
1	Professor W. R. Sears, Graduate School of Aeronautical Engineering, Cornell University, Ithaca, New York.
1	Mr. George H. Pedersen, Curtiss-Wright Corporation, Wright Aeronautical Division, Wood-Ridge, New Jersey, Location CC-1 Engrg. Mezz.
1	Mr. G. Tedrew, Food Machinery Corporation, P. O. Box 367, San Jose, California.
1	General Applied Science Laboratory, Merrick and Stewart Avenues, Westbury, Long Island, New York, Attn: Dr. Frank Lane.
1	Mr. R. McCandliss, Electric Boat Division, General Dynamics Corporation, Groton, Connecticut.
1	Dr. A. S. Iberall, President, General Technical Services, Inc., 2640 Whiton Road, Cleveland 18, Ohio.
1	Gibbs and Cox, Inc., 21 West Street, New York, New York 10006.
1	Mr. Eugene F. Baird, Chief of Dynamic Analysis, Grumman Aircraft Engineering Corporation, Bethpage, Long Island, New York.
1	Mr. Robert E. Bower, Chief, Advanced Development, Grumman Aircraft Engineering Corporation, Bethpage, Long Island, New York.
1	Mr. William P. Carl, Grumman Aircraft Engineering Corporation, Bethpage, Long Island, New York.
1	Grumman Aircraft Engineering Corporation, Research Department, Plant 25, Bethpage, Long Island, New York 11714, Attn: Mr. Kenneth Keen.
1	Dr. O. Grim, Hamburgische Schiffbau-Versuchsanstalt, Bramfelder Strasse 164, Hamburg 33, Germany.
1	Dr. H. W. Lerbs, Hamburgische Schiffbau-Versuchsanstalt, Bramfelder Strasse 164, Hamburg 33, Germany.
1	Dr. H. Schwanecke, Hamburgische Schiffbau-Versuchsanstalt, Bramfelder Strasse 164, Hamburg 33, Germany.
1	Professor G. P. Weinblum, Director, Institute for Schiffbau, University of Hamburg, Berliner Tow 21, Hamburg, Germany.
1	Professor G. F. Carrier, Harvard University, Cambridge 38, Massachusetts.
1	Dr. S. F. Hoerner, 148 Busteed Drive, Midland Park, New Jersey.
1	Mr. P. Eisenberg, President, Hydronautics, Incorporated, Pindell School Road, Howard County, Laurel, Maryland.
1	Professor Carl Prohaska, Hydro-og Aerodynamisk Laboratorium, Lyngby, Denmark.

Copies	Organization
1	Professor L. Landweber, Iowa Institute of Hydraulic Research, State University of Iowa, Iowa City, Iowa.
1	Professor H. Rouse, Iowa Institute of Hydraulic Research, State University of Iowa, Iowa City, Iowa.
1	Professor S. Corrsin, Department of Mechanics, The Johns Hopkins University, Baltimore 18, Maryland.
2	Professor O. M. Phillips, Division of Mechanical Engineering, Institute for Cooperative Research, The Johns Hopkins University, Baltimore 18, Maryland.
1	Mr. Bill East, Lockheed Aircraft Corporation, California Division, Hydrodynamics Research, Burbank, California.
1	Mr. R. W. Kermeen, Lockheed Missiles and Space Company, Department 81-73/Bldg. 538, P.O. Box 504, Sunnyvale, California.
1	Department of Naval Architecture and Marine Engineering, Room 5-228, Massachusetts Institute of Technology, 77 Massachusetts Avenue, Cambridge 39, Massachusetts.
1	Professor M. A. Abkowitz, Massachusetts Institute of Technology, Cambridge 39, Massachusetts.
1	Professor H. Ashley, Massachusetts Institute of Technology, Cambridge 39, Massachusetts.
1	Professor A. T. Ippen, Massachusetts Institute of Technology, Cambridge 39, Massachusetts.
1	Professor M. Landahl, Massachusetts Institute of Technology, Cambridge 39, Massachusetts.
1	Dr. H. Reichardt, Director, Max-Planck Institut fur Stromungsforschung, Bottingerstrasse 6-8, Gottingen, Germany.
1	Professor R. B. Couch, University of Michigan, Ann Arbor, Michigan.
1	Professor W.W. Willmarth, University of Michigan, Ann Arbor, Michigan.
1	Midwest Research Institute, 425 Volker Boulevard, Kansas City, Missouri, Attn: Library.
1	Director, St. Anthony Falls Hydraulic Laboratory, University of Minnesota, Minneapolis 14, Minnesota.
1	Dr. C. S. Song, St. Anthony Falls Hydraulic Laboratory, University of Minnesota, Minneapolis 14, Minnesota.
1	Mr. J. M. Wetzel, St. Anthony Falls Hydraulic Laboratory, University of Minnesota, Minneapolis 14, Minnesota.

Copies	Organization
1	Head, Aerodynamics Division, National Physical Laboratory, Teddington, Middlesex, England.
1	Mr. A. Silverleaf, National Physical Laboratory, Teddington, Middlesex, England.
1	The Aeronautical Library, National Research Council, Montreal Road, Ottawa 2, Canada.
1	Dr. J. B. Van Manen, Netherlands Ship Model Basin, Wageningen, The Netherlands.
1	Professor John J. Foody, Chairman, Engineering Department, State University of New York, Maritime College, Bronx, New York 10465.
1	Professor J. Keller, Institute of Mathematical Sciences, New York University, 25 Waverly Place, New York 3, New York.
1	Professor J. J. Stoker, Institute of Mathematical Sciences, New York University, 25 Waverly Place, New York 3, New York.
1	Dr. T. R. Goodman, Oceanics, Incorporated, Technical Industrial Park, Plainview, Long Island, New York.
1	Professor J. William Holl, Department of Aeronautical Engineering, The Pennsylvania State University, Ordnance Research Laboratory, P.O. Box 30, University Park, Pennsylvania.
1	Dr. M. Sevik, Ordnance Research Laboratory, Pennsylvania State University, University Park, Pennsylvania.
1	Dr. George F. Wislicenus, Garfield Thomas Water Tunnel, Ordnance Research Laboratory, The Pennsylvania State University, P.O. Box 30, University Park, Pennsylvania 16801.
1	Mr. David Wellinger, Hydrofoil Projects, Radio Corporation of America, Burlington, Massachusetts.
1	The Rand Corporation, 1700 Main Street, Santa Monica, California, 90406, Attn: Library.
1	Professor R. C. DiPrima, Department of Mathematics, Rensselaer Polytechnic Institute, Troy, New York.
1	Mr. L. M. White, U. S. Rubber Company, Research and Development Department, Wayne, New Jersey.
1	Professor J. K. Lunde, Skipsmodelltanken, Trondheim, Norway.
1	Editor, Applied Mechanics Review, Southwest Research Institute, 8500 Culebra Road, San Antonio 6, Texas.
1	Dr. H. N. Abramson, Southwest Research Institute, 8500 Culebra Road, San Antonio 6, Texas.

Copies	Organization
1	Mr. G. Ransleben, Southwest Research Institute, 8500 Culebra Road, San Antonio 6, Texas.
1	Professor E. Y. Hsu, Stanford University, Stanford, California.
1	Dr. Byrne Perry, Department of Civil Engineering, Stanford University, Stanford, California 94305.
1	Dr. J. P. Breslin, Stevens Institute of Technology, Davidson Laboratory, Hoboken, New Jersey.
1	Mr. D. Savitsky, Stevens Institute of Technology, Davidson Laboratory, Hoboken, New Jersey.
1	Mr. S. Tsakonas, Stevens Institute of Technology, Davidson Laboratory, Hoboken, New Jersey.
1	Dr. Jack Kotik, Technical Research Group, Inc., Route 110, Melville, New York.
1	Dr. R. Timman, Department of Applied Mathematics, Technological University, Julianalaan, 132, Delft, Holland.
1	The Transportation Technical Research Institute, Investigation Office, Ship Research Institute, 700 Shinkawa, Mitaka, Tokyo-to, Japan.
1	Dr. Grosse, Versuchsanstalt fur Wasserbau und Schiffbau, Schleuseninsel im Tiergarten, Berlin, Germany.
1	Dr. S. Schuster, Director, Versuchsanstalt fur Wasserbau und Schiffbau, Schleusensinsel im Tiergarten, Berlin, Germany.
1	Technical Library, Webb Institute of Naval Architecture, Glen Cove, Long Island, New York.
1	Professor E. V. Lewis, Webb Institute of Naval Architecture, Glen Cove, Long Island, New York.
1	Mr. C. Wigley, Flat 103, 6-9 Charterhouse Square, London E. C. 1, England.
1	Coordinator of Research, Maritime Administration, 441 G Street, NW, Washington 25, D. C.

Unclassified

Security Classification

DOCUMENT CONTROL DATA - R&D

(Security classification of title, body of abstract and indexing annotation must be entered when the overall report is classified)

1. ORIGINATING ACTIVITY *(Corporate author)*
St. Anthony Falls Hydraulic Laboratory, University of Minnesota

2a. REPORT SECURITY CLASSIFICATION
Unclassified

2b. GROUP

3. REPORT TITLE
MEASUREMENTS OF THE LEADING-EDGE SEPARATION BUBBLE FOR SHARP-EDGED HYDROFOIL PROFILES

4. DESCRIPTIVE NOTES *(Type of report and inclusive dates)*
Final Report

5. AUTHOR(S) *(Last name, first name, initial)*
Wetzel, J. M. and Foerster, K. E.

6. REPORT DATE	7a. TOTAL NO. OF PAGES	7b. NO. OF REFS
June 1966	28	5

8a. CONTRACT OR GRANT NO.	9a. ORIGINATOR'S REPORT NUMBER(S)
Nonr 710(47)	Project Report No. 83
b. PROJECT NO.	
c.	9b. OTHER REPORT NO(S) *(Any other numbers that may be assigned this report)*
d.	

10. AVAILABILITY/LIMITATION NOTICES
Distribution of this document is unlimited.

11. SUPPLEMENTARY NOTES	12. SPONSORING MILITARY ACTIVITY
	Office of Naval Research

13. ABSTRACT

Measurements were made of the leading edge separation bubble for sharp-edged profiles of finite span submerged below a free surface. These hydrofoils were tested under a fully-wetted flow condition. Flow visualization techniques were used to determine the separation region primarily as a function of velocity, chord length, profile shape, aspect ratio, and angle of attack. The bubble length increased with increasing angle of attack and aspect ratio. An increase in the wedge angle for wedged shaped profiles required an increase in angle of attack to attain the same bubble length. Variation of the chord length and leading-edge thickness had little effect on the ratio of bubble to chord length.

DD FORM 1 JAN 64 1473 0101-807-6800

Unclassified

Security Classification

14. KEY WORDS	LINK A		LINK B		LINK C	
	ROLE	WT	ROLE	WT	ROLE	WT
Hydrofoils						
Flow Visualization						
Separation						

INSTRUCTIONS

1. ORIGINATING ACTIVITY: Enter the name and address of the contractor, subcontractor, grantee, Department of Defense activity or other organization *(corporate author)* issuing the report.

2*a*. REPORT SECURITY CLASSIFICATION: Enter the overall security classification of the report. Indicate whether "Restricted Data" is included. Marking is to be in accordance with appropriate security regulations.

2*b*. GROUP: Automatic downgrading is specified in DoD Directive 5200.10 and Armed Forces Industrial Manual. Enter the group number. Also, when applicable, show that optional markings have been used for Group 3 and Group 4 as authorized.

3. REPORT TITLE: Enter the complete report title in all capital letters. Titles in all cases should be unclassified. If a meaningful title cannot be selected without classification, show title classification in all capitals in parenthesis immediately following the title.

4. DESCRIPTIVE NOTES: If appropriate, enter the type of report, e.g., interim, progress, summary, annual, or final. Give the inclusive dates when a specific reporting period is covered.

5. AUTHOR(S): Enter the name(s) of author(s) as shown on or in the report. Enter last name, first name, middle initial. If military, show rank and branch of service. The name of the principal author is an absolute minimum requirement.

6. REPORT DATE: Enter the date of the report as day, month, year; or month, year. If more than one date appears on the report, use date of publication.

7*a*. TOTAL NUMBER OF PAGES: The total page count should follow normal pagination procedures, i.e., enter the number of pages containing information.

7*b*. NUMBER OF REFERENCES: Enter the total number of references cited in the report.

8*a*. CONTRACT OR GRANT NUMBER: If appropriate, enter the applicable number of the contract or grant under which the report was written.

8*b*, 8*c*, & 8*d*. PROJECT NUMBER: Enter the appropriate military department identification, such as project number, subproject number, system numbers, task number, etc.

9*a*. ORIGINATOR'S REPORT NUMBER(S): Enter the official report number by which the document will be identified and controlled by the originating activity. This number must be unique to this report.

9*b*. OTHER REPORT NUMBER(S): If the report has been assigned any other report numbers *(either by the originator or by the sponsor)*, also enter this number(s).

10. AVAILABILITY/LIMITATION NOTICES: Enter any limitations on further dissemination of the report, other than those imposed by security classification, using standard statements such as:

(1) "Qualified requesters may obtain copies of this report from DDC."

(2) "Foreign announcement and dissemination of this report by DDC is not authorized."

(3) "U. S. Government agencies may obtain copies of this report directly from DDC. Other qualified DDC users shall request through _____."

(4) "U. S. military agencies may obtain copies of this report directly from DDC. Other qualified users shall request through _____."

(5) "All distribution of this report is controlled. Qualified DDC users shall request through _____."

If the report has been furnished to the Office of Technical Services, Department of Commerce, for sale to the public, indicate this fact and enter the price, if known.

11. SUPPLEMENTARY NOTES: Use for additional explanatory notes.

12. SPONSORING MILITARY ACTIVITY: Enter the name of the departmental project office or laboratory sponsoring *(paying for)* the research and development. Include address.

13. ABSTRACT: Enter an abstract giving a brief and factual summary of the document indicative of the report, even though it may also appear elsewhere in the body of the technical report. If additional space is required, a continuation sheet shall be attached.

It is highly desirable that the abstract of classified reports be unclassified. Each paragraph of the abstract shall end with an indication of the military security classification of the information in the paragraph, represented as *(TS)*, *(S)*, *(C)*, *or (U)*.

There is no limitation on the length of the abstract. However, the suggested length is from 150 to 225 words.

14. KEY WORDS: Key words are technically meaningful terms or short phrases that characterize a report and may be used as index entries for cataloging the report. Key words must be selected so that no security classification is required. Identifiers, such as equipment model designation, trade name, military project code name, geographic location, may be used as key words but will be followed by an indication of technical context. The assignment of links, roles, and weights is optional.